Master of Science Thesis

BNCT in vivo dosimetry: A feasibility study using an HPGe detector for prompt gamma spectroscopy

Carl Östlund

Supervisors: Crister Ceberg & Per Munck af Rosenschöld

Medical Radiation Physics
Clinical Sciences,Lund
Lund University, 2005

Abstract

Increased accuracy in patient dosimetry in BNCT is needed. This need for more accurate individual patient dose estimations initiated this project at the Swedish BNCT facility at Studsvik. One possible way to achieve this is to use an HPGe detector. This project involves the complete construction and testing of such a system in a treatment representative environment.

The system builds on an ORTEC GMX10 Germanium detector, viewing only a limited part of the patients head from inside the treatment room. The detector configuration needs shielding from neutrons and photons. Sufficient shielding has been achieved through the making of special lithium plastic which removes the neutron fluence within the detector crystal. Lead was used to shield the detector from photons.

The test measurements performed in Studsvik showed that it was possible to use the detector in the environment and to measure a spectrum at a fairly high nominal reactor power.
The measurements have been performed at 1-100 kW nominal reactor power on a cubic phantom (140x180x170 mm) filled with a mix of water and boric acid. Unexpected high count rates up to 300000 cps at 100kW caused problems in spectrum analysis which showed a small boron peak originating from the phantom but also a high background. The initial signal to noise ratio showed to be very low, close to 0 and by improving the structural design of the detector shielding, great improvements in suppressing the background have been made and as a result of this higher signal to noise ratio of 0.1 was achieved with a low peak count rate of 28 cps. In order to be able to increase signal to noise ratio to reach clinical accuracy further improvements are needed. In present state the detector equipment is capable of measuring a boron peak at a clinically relevant reactor power, originating from a patient head.

Introduction

Boron Neutron Capture Therapy (BNCT) is a form of radiation therapy that use the neutron capture in boron to treat in this case, a tumour seated in the brain tissue. The absorbed dose to the tumour is a combination of neutron reactions in tissue and gammas produced in the reactor and beam filter. An accurate dose determination in mixed radiation fields is more difficult compared to conventional radiotherapy. The uncertainty in boron uptake and dose contribution needs to be decreased. Today the standard method for estimation of the boron concentration in brain tissue is by using blood samples and pre-determined brain-to-blood concentration ratios. Improved boron uptake measurements at the time of the treatment are needed especially in order to accurately establish the dose-response relationship; otherwise the scientific value of the future clinical trials will be limited.

Clinical BNCT dosimetry

Going through BNCT therapy treatment a patient is exposed to more than one absorbed dose component. These different absorbed dose components have different radiobiological effectiveness (Coderre and Morris, 1999), which needs to be taken in to account in clinical dosimetry. The method of assigning a unique weight factor to each dose component that corresponds directly to the relative biological effectiveness (RBE) has been adopted in the trial at the Studsvik facility (Capala et al, 2003). A total absorbed dose can be calculated as a weighted sum of the different components:

$$D_{Total} = D_{Boron} \cdot w_{Boron} + D_{\gamma} \cdot w_{\gamma} + D_{Fast} \cdot w_{Fast} + D_{N} \cdot w_{N} \qquad \text{(Eq. 1)}$$

where D_{Total} is the total absorbed dose given in often denoted Gy(w), $D_{Boron} \cdot w_{Boron}$ is the weighted dose contribution from the neutron capture in boron, $D_{\gamma} \cdot w_{\gamma}$ is the weighted photon absorbed dose, $D_{Fast} \cdot w_{Fast}$ is the weighted absorbed dose from fast neutrons and $D_{N} \cdot w_{N}$ is the weighted contribution of the absorbed dose delivered by neutron capture reactions in nitrogen.
These weight factors w (for healthy brain tissue), has been investigated for the BPA (boronophenylalanine) compound in animal experiments and has been set to: $w_{Boron} = 1.3$, $w_{\gamma} = 1.0$, $w_{Fast} = 3.2$, $w_{N} = 3.2$ and the weight factor for tumour tissue, $w_{boron,tumour} = 3.8$. The founding idea is that the tumour will concentrate BPA and when irradiated the tumour receives a higher dose than the healthy brain tissue. The BPA concentration can be up to 4 times higher than in the blood stream and healthy brain tissue (Coderre et al, 1993 and 1994, Coderre and Morris, 1999). The amounts of boron accumulated in the tumour cells are very individual (Elowitz et al, 1998) and the boron absorbed dose component can be derived from the following expression:

$$D_{Boron} = C_{B} \cdot \phi_{th} \cdot KF_{B} \qquad \text{(Eq. 2)}$$

Where C_{B}, is the boron concentration by weight in tissue, ϕ_{th} is the thermal neutron fluence and KF_{B} is the kerma factor for ^{10}B. In clinical practice there are often large uncertainties in C_{B}^{brain}.

Prompt Gamma Spectroscopy

In order to perform non-invasive in vivo dosimetry, one can use the boron-neutron reaction prompt gamma with the energy of 478 keV to make an estimation of the boron concentration in a selected volume of the brain. The boron peak of 478 keV is not the only photon energy in a BNCT treatment gamma spectrum, thermal neutron capture in hydrogen contributes with a large peak at 2223 keV and nitrogen contributes with the gamma lines 1678, 1885 keV, intensities 7 and 22 percent. Nitrogen also contributes to a measured spectrum with several gamma lines above 3500 keV, for example 3332, 3677, 4508, 5269, 5297, 5562, 6322, 7299 keV with the corresponding intensities 10, 16, 30, 21, 18, 10, 17 and 9 percent. Almost all elements in the periodic table have gamma lines produced by thermal neutron capture but only a few with sufficient intensity will be visible in a measured spectrum during treatment.
In Petten, the Netherlands, a functional system for prompt-gamma spectroscopy (PGS) was developed using an HPGe detector (High Purity Germanium detector), called gamma ray telescope (Verbakel et al, 2001, Munck af Rosenschöld et al, 2001).
In Japan several investigations in this field, PG-Spect have been performed and different systems has been evaluated. Matsumoto and Aizawa (1990) used a germanium detector to measure the prompt gamma rays emitted from a sample placed in a silicon crystal filtered thermal neutron beam. This was an attempt to create a high purity beam consisting out of thermal neutrons, and this in an attempt trying to detect low concentrations of boron in small samples. Mukai, Nakagawa and Matsumoto et al (1995) developed a system that measured prompt boron gammas in rabbit brains irradiated with a narrow thermal neutron beam of diameter 5 mm through a drilled hole in the rabbits cranial bone. They used a germanium detector (Si implanted) to do their spectrum measurements. Kobayashi et al (2000) evaluated a theoretical system using an array of detectors placed behind 20 cm of tungsten with 2mm collimator holes placed in a circular pattern around the patients head during therapy. The BNCT facility in Petten is the only facility that has tried and succeeded using the gamma ray telescope for online measurement of the boron concentration in patients (Verbakel et al, 2003). The system is operational at present time, but requires large efforts in post irradiation reconstruction and evaluation. The system estimates an average boron concentration in a relative large volume of the head.

Aim of this thesis

-to design and construct a prompt gamma spectroscopy (PGS) system for the Studsvik BNCT facility.

-to determine if the detector system is feasible for in vivo patient measurements.

-to discuss further improvements towards increased clinical utility.

Background

Several trials on BNCT treatment of glioblastoma multiforme (GBM) commenced during the later part of the1900: s. At Brookhaven National Laboratory (BNL) in collaboration with Massachusetts Institute of Technology (MIT), a clinical trial was started already in the 1950s, using the MIT reactor facility. The results of this trial were not satisfying, due to poor neutron penetration and ineffective boron carrier compounds. The poor penetration led to severe complications in the skin when trying to treat deeper

seated tumours in the brain. These effects and results led to discontinuation of the trial. (Asbury et al, 1972**)**
In Japan at the Hitachi research reactor a study was initiated in 1968. This study had a different approach compared to the approach of the trial at Brookhaven USA. In this trial a compound called BSH (Sodium mercaptoundecahydro-closo-dodecarborate) was used. The radiation treatment was performed intra-operatively (with cranial bone was temporarily removed).
During the 1990s five BNCT facilities; Hitachi research reactor, Japan, in Petten, the Netherlands, VTT, Finland, BNL and MIT (two separate trials), USA, all hosted ongoing clinical trials. In 1999 a clinical trial in Finland at VTT (Technical research centre of Finland) was initiated and in 2001 the study started in Studsvik, Sweden started.
In Sweden approximately 250 people get diagnosed with Glioblastoma Multiforme every year. This constitutes roughly 0.5% of all diagnosed cancers reported in one year in Sweden. The survival to deceased ratio of the patients treated for this disease is close to zero (Gilbert et al, 2002). Glioblastoma multiforme is an infiltrative brain tumour that grows aggressively. This type of tumour consists of a dense cluster of cells, but also infiltrates the surrounding tissue by spreading out single cells. The growth pattern and the low radio-sensitivity decimate the ways of treatment. The most used treatment today for this type of cancer is extensive radiotherapy combined with both chemotherapy and surgery. With BNCT the goal is to target and strike out both the remaining gross tumour and single cells at once by using selective boron carriers. The treatment in Sweden is performed post operation at which as large as possible amount of tumour is removed.

From reactor to tumour cell

The Studsvik neutron beam is an epithermal beam with an energy range of approximately 0.4-20 keV. The neutron energy spectrum differs between different facilities, which can be explained mainly by differences in reactor cores and beam filter configurations.
The beam filter is composed out of materials that are placed in a specific order to moderate fast neutrons and also to filter out lower unsuitable energies in the core neutron spectrum. The order of these material slabs is at the same time chosen to suppress the photon background as much as possible. From the fission process in the reactor core the filter creates the desired epithermal neutron energy spectrum used in the beam. The reason why an epithermal beam is used is the increase of the depth of the thermal neutron fluence maximum compared to a thermal neutron beam. When a thermal neutron approaches a ^{10}B atom and passing by the nucleus in a range of a few fm, the neutron faces the chance of absorption, due to the high thermal capture cross section of 3838 barns at 0.0253 eV (ENDF/60).
When absorbed it contributes to instability in the boron nucleus that the will undergo prompt fission, and photon emission (478 keV) as a result in 94 % of the cases. In the other 6 % of the cases there is no emission of gamma. The ^{11}B nucleus is divided into two fragments, ^{7}Li and ^{4}He. The following equations show the reactions.

$$1.\ {}^{10}B + n \rightarrow {}^{11}B^{*} \rightarrow {}^{7}Li + \alpha + \gamma$$
$$2.\ {}^{10}B + n \rightarrow {}^{11}B^{*} \rightarrow {}^{7}Li + \alpha \qquad \text{(Eq. 3, 4)}$$

The energy of the two fission fragments is 1.47 MeV for the helium nucleus and 0.84 MeV for the recoiling lithium nucleus. The ranges of the two fragments in tissue are approximately 9 μm and 5 μm in the case of photon emission. The total path-length is roughly one cell diameter.

When the ^{10}B atom absorbs a neutron and undergoes prompt fission described by the equations above, and the event takes place near a cell core, the damage is severe. The fragments will ionize atoms in its path, creating δ-particles and cause damage representative of a high LET particle.

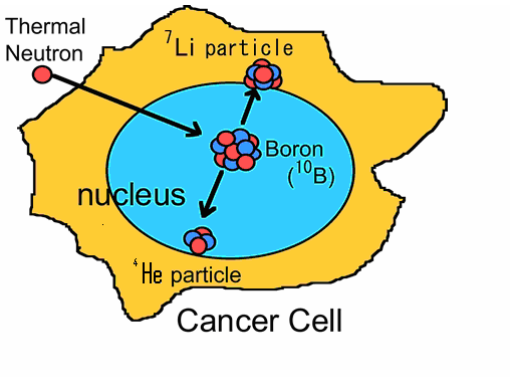

Figure 1. *A thermal neutron absorbed by a boron nucleus undergoes prompt fission*

Boron biodistribution

BNCT is a method that uses tumour cell biology and characteristics in a treatment beneficial way. One approach is to use the increased tumour nutrition need to deliver dose in therapy. The boron (^{10}B) can be accumulated in the tumour cells using a boron compound that is targeting cells in great need of nutrition. A different way is to use the disruption of the blood-brain barrier to load up the tumour with boron.
The boron carrier compound is administrated by direct infusion in the blood stream. Due to diffusion and other mechanisms the boron concentration in the healthy brain cell is considered to be the same or less compared to the concentration in the blood stream (Elowitz et al, 1998).
Investigations of the biodistribution of the boron compound BSH (Sodium mercaptoundecahydro-closo-dodecarborate) in patients with astrocytoma Grade III and IV, demonstrated a heterogeneous boron uptake in the tumour (Ceberg et al, 1995). This grade of malignity is considered equivalent to Glioblastoma Multiforme in aspect of boron uptake (Burger et al, 1985).
This has also been investigated and suggested by Ono et al (1996) with data from a rat model and Coderre et al (1998) also found heterogeneous tumour uptake for BPA. Heterogeneous gross tumour BPA boron uptake was shown by Smith et al (2002) for two different infusion times, 2 and 6 hours. In clinical practice a blood sample from the patient is analyzed for boron concentration and this will later be used as a correction for the monitor units planned for the treatment in question. A 1:1 boron concentration ratio between healthy brain tissue and blood is used (Palmer et al, 2002; Capala et al, 2003) and this introduces uncertainties in calculated dose to the irradiated volume in the individual patient. If boron concentration would be higher in the brain tissue than in the blood stream this would decrease the thermal neutron fluence with increased depth in the brain tissue more than expected, the boron would work as an attenuator. This means a lower absorbed dose in deeper seated regions and incorrect calculated absorbed dose values in this region.

Materials and methods

Detector system

The detector used was an Ortec GMX10 n-type HPGe detector. We have chosen an n-type detector since it is more resistent to neutron irradiation. In order to handle the high count rates expected in the detector setup, a digital multi channel analyzer (MCA), DSPEC^{plus} system was chosen.

Radiation shielding

The construction of the radiation shielding is divided into two parts. Shielding of neutrons and shielding of photons. The aim of the neutron shielding was to moderate the non thermal neutrons that scatter on to the detector construction and absorb them. ^{6}Li is a material that has a high thermal neutron cross section of 980 barn (ENDF/60), and with the desirable quality of not releasing any prompt or activation gammas. The natural abundance is 6.7%. It was decided to use 5 mm of grinded lithium powder, to stop the thermal neutrons. A 17 mm thick PMMA plastic shielding was manufactured. PMMA has a high hydrogen concentration, around 10^{22} atoms/cm^{3}.
Mixing the lithium powder with the powder component of PMMA, ^{6}Li was evenly distributed through the plastic body. The mix consisted of 30% lithium powder and 70% plastic (numbers are given in weight percentage).

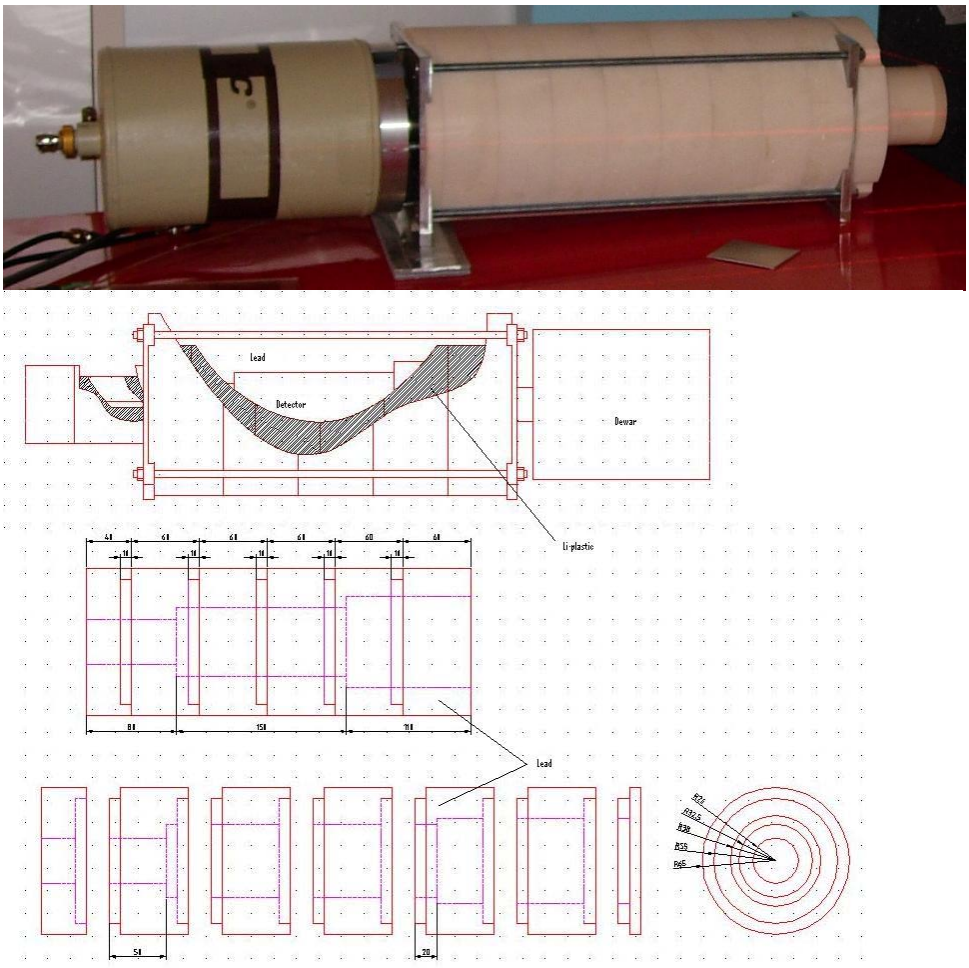

Figure 2.1, 2.2. *Above: The neutron shielding PMMA plastic, mixed with 30% lithium carbonate mounted outside of the lead.*
Below: Principle drawing of the detector construction.

The photon shielding and collimator was constructed out of lead. The lead shielding rings were folded together inside the neutron shielding. The collimator was to project a surface from a representative volume at a given distance. The thickness of the front lead was 80 mm, leaving the detector with 1.6% penetration of the hydrogen photons. The collimator itself functions as a shielding. A set of cylindrical lead plates with a centred 10 mm diameter hole was manufactured, total length of 38 cm. This collimator made it possible to vary the area of projection in order to find a suitable setup.
In order to prevent damage to the detector crystal a 1 mm polyethylene bushing was placed over the front cap, spaced 5 mm.

Figure 3. *The manufactured lead shielding disassembled showing the frontal polyethylene bushing protecting the fragile beryllium window. A different collimator manufactured for tomographical purpose is shown at the bottom of the picture.*

Monte Carlo calculations

The Monte Carlo code MCNP (version 4c2) was used to investigate the detector and shielding preformance inside the treatment room. The aim of the calculations was to estimate

i) Geometrical efficiency
ii) Actual count rate inside the BNCT treatment room at Studsvik using the complete geometry of the beam filter and beam collimator.

The detector geometry was inserted in a way representative of a treatment situation. In order to be able to calculate the actual count rate, the following approach was made. The method was to estimate the count rate by several different steps in calculation. The first step of the calculation was to estimate the photon fluence emerging from neutron capture reactions in a phantom, size 18, 14, 17 cm (length, width, and height) filled with water and boric acid.
To do this correctly the photon production in cells outside the phantom was turned off.

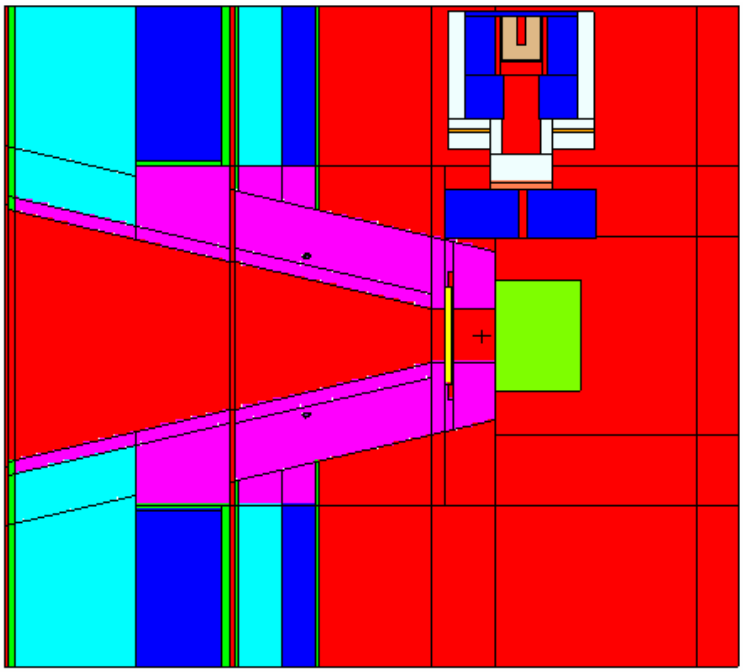

Figure 4 The *complete MCNP geometry used visualized in vised 4C2. The beam collimator is the pink conical shape to the left in the image and the surrounding structure is the treatment room wall. The detector is the blue and white structure at the top and the phantom is the green rectangular shaped structure close to the beam collimator.*

The connection between the measured fluence and unnormalized calculated fluence is given by the following equation.

$$\Phi_{ph} = \Phi_{MC_1} \cdot C_1 \qquad \text{(Eq. 5)}$$

Where Φ_{MC_1} is the calculated photon fluence, Φ_{ph} the real photon fluence, and C_1 is a normalisation factor determined through previous experiments for 1 MW nominal reactor power (Giusti et al, 2003).

The next step was to construct a new photon source from the results of the first calculation. The fluence was recalculated in the whole phantom using the new source that was uniformly sampled inside the phantom. This was done to estimate the difference in photon fluence between use of the neutron source and the new photon source. This value was later used to normalise the obtained value of the actual count rate.

The final step was to calculate the detector count rate using the new photon source. The actual count rate was given by the unnormalized MCNP value multiplied with the previously mentioned source normalisation factor.
In order to better fit the value to the real situation where neutron fluence is decreasing along beam axis through the phantom, an fluence correction ratio estimation was made. This was done with a set of two new photon fluence calculations using the neutron source. The first calculation giving the fluence value in the whole of the phantom and the second calculation giving the value from the conical volume projected on the detector volume through the collimator hole. The correction factor (k) is given by

$$k = \frac{\Phi_{projection}}{\Phi_{phantom}} \qquad \text{(Eq. 6)}$$

Measurements

Measurements were performed to experimentally determine
i) the geometrical efficiency.
ii) the actual count rate inside the treatment room at Studsvik.

The geometric efficiency of the detector with the shielding and collimator applied was tested using a ^{137}Cs point source with the activity of 47 MBq. In steps of 1 mm the source was moved along the horizontal axis perpendicular to the collimator axis. The measuring time was set to 300 seconds live time for each position. The extension of the source capsule was 3.0 mm.

Count rate measurements were performed at the Studsvik treatment facility. The measurement was set up as a fixed geometry measurement. The position of the detector was perpendicular to the beam axis and in the horizontal plane crossing the beam axis. The measurement distance was set to 83 cm between detector surface and neutron beam axis and the short side of the cubic shaped phantom was facing the detector.

Figure 5. *The pictures show the measurement setup at Studsvik inside the treatment room.*

Tomography

Additional experiments were made in order to investigate potential future developments to increase the clinical utility of the PGS-system.
For instance, one interesting line of investigation is to study if it is possible to quantify the boron uptake in a tomographical image, and with what errors.
In order to investigate this, a very simple model for this kind of measurements was made, consisting of a cylindrical PMMA phantom filled with water. Inside the phantom a hollow PMMA sphere also filled with water was placed off centre. These cavities were filled with ^{131}I in a concentration order of 10 to 1 in favour of the sphere. The diameter of the sphere was 20 mm. The diameter of the phantom was 105 mm.

Figure 6. *The tomographical setup. Left picture showing the setup from the right. Right picture showing the phantom and rotation board from above.*

A different type of lead collimator was used for this experiment, to narrow the field of view in order to receive better spatial resolution. By measuring along a path perpendicular to the collimator axis with 5 mm spacing between the measuring points, a single angular projection was measured. Each projection was built up by 22 steps with the measuring time of 300 s live time each. In total 16 angles were measured. The resulting values obtained from the photo peak in each point served as a pixel value in the projection vector. Due to the large consumption of time all projections needed to be corrected for radioactive decay. This was done prior to the reconstruction. The methods used for reconstruction were FBP (**F**iltered **B**ackward **P**rojection) and MLEM (**M**aximum **L**ikelihood **E**xpectation **M**aximization).

Results

Radiation shielding

The detector and electronics showed that it was capable of high count rates up to 140 kcps, without a decrease in energy resolution. FWHM did not exceed 3% for the 511 keV peak at 140 kcps. No indication of fast neutron damage was observed after measurements inside the treatment room. Energy recalibration of the detector had to be performed numerous times due to changes in settings of the MCA.
The lead shielding showed to be well dimensioned in the front but penetrations through the sides were discovered through the large background present in the measured spectrum. The manufactured neutron shielding worked satisfactory and no damage to the crystal could be observed in the spectrum. This would be visible as irregularities in the photo peak shape such as an additional shoulder on the left side of the peak.
No unusually high dead time or any other unusual behaviour was observed which could be an indicator of fast or epithermal neutron fluence trough the detector crystal.

Monte Carlo calculations

Geometrical Efficiency

The MCNP estimation of the geometrical efficiency gave a conical shaped detector response. The values were normalised to show the similarity between the two curves below.

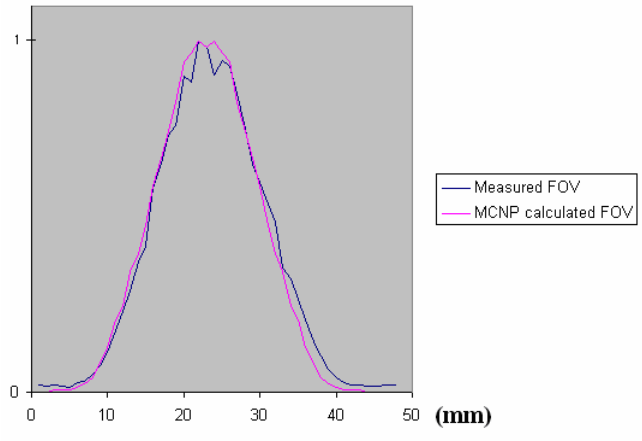

Figure 7. *Comparison of measured and calculated FOV using the topographic collimator in estimation of geometrical efficiency, the results are normalized. The statistical uncertainty of the MC-calculation was less than 0.15% in all points (1 s.d.)*

Actual count rate

From MCNP results the relative efficiency was determined to be 26%, which is 44% higher than the ORTEC detector specifications.
The attempt to estimate count rate built up on a series of calculations resulted in a calculated fluence of $1.21 \cdot 10^8 \gamma / s \cdot cm^2$, presented as an average fluence in the whole phantom volume. Use of the above calculated fluence the count rate resulted in a non corrected count rate of 146600 cps at 600 kW. Corrected with the fluence correction factor k=1.81 the final count rate was determined to be 265000 cps.

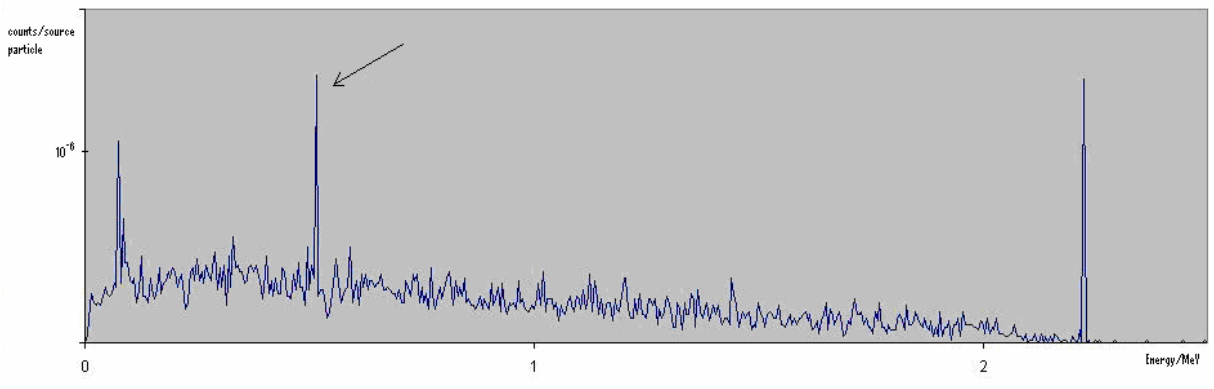

Figure 8. *Picture showing a calculated spectrum. Arrow pointing out the 511 keV peak. The large variations in the background are the result from poor statistics. (Scales are linear)*

Measurements

Geometrical Efficiency

Results are shown together with the MC results in fig. 7.
The FWHM was estimated to 16 mm.

Actual count rate

The detector was operational up to 100 kW nominal reactor power corresponding to 290 000 cps before 100% dead time was reached. The spectrum below suffered from large background. Therefore the spectrum measurements were made at 1 kW nominal reactor power to measure with low dead time to minimize the background interference of the boron peak. The count rate in the boron peak was 28 cps.

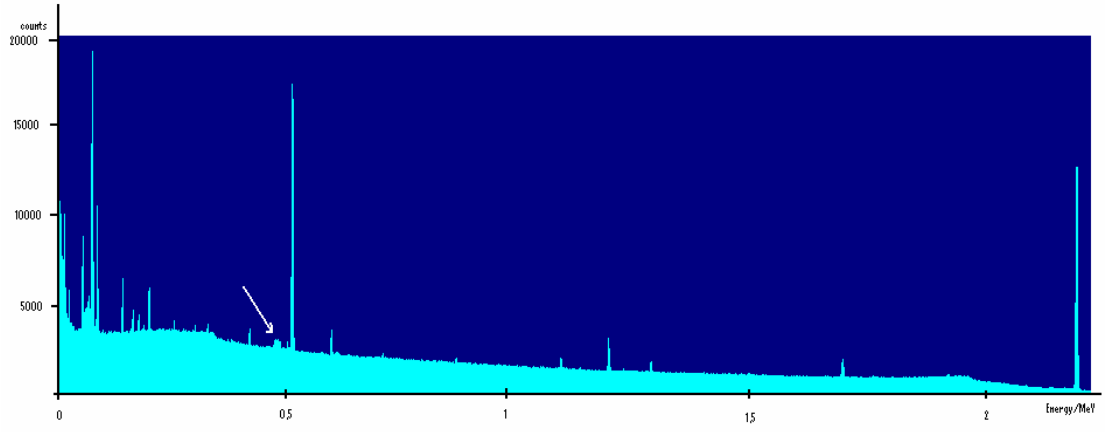

Figure 9. *The arrow is pointing out the measured boron peak in Studsvik. The detector*

is viewing roughly the whole phantom. (Livetime 213s and 24% deadtime, scales are linear.)

Tomography

The uncertainty in peak area calculation by the software was between 6% and 41%, where the high value represents the endpoint measurement positions of the projection. The concentration relation of 10:1 is not achieved between the different activity concentration regions in the MLEM image which reveals a ratio close to 5:1. The FBP image reveals a smaller ratio close to 4:1.

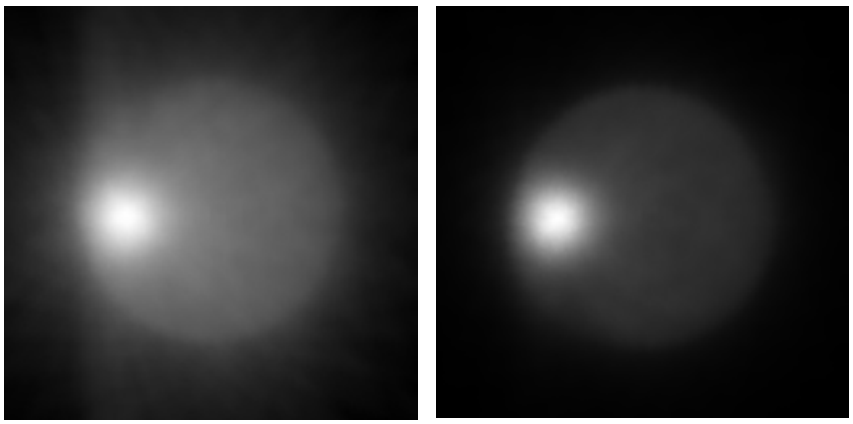

Figure 10. *The left picture is showing the data set reconstructed with FBP and the right picture showing the same data set reconstructed with MLEM*

Discussion

Detector system and shielding

The choice of equipment regarding function proved to be adequate. The electronics proved to be able to handle the high count rate, this making it possible to bring the detector inside the treatment room. There were difficulties in estimations of the exact count rate due to fluctuations and discrimination levels affecting the integral of the spectrum, but the observed limit in count rate was estimated to be 140 000 +/- 15 000 cps. The equipment did not show any damage caused by the fitting of the manufactured shielding parts around the detector. Inside the shielding the detector casing was free from contact with any part of the surrounding components.

The manufactured neutron shielding proved to work satisfactory. After 15 minutes of irradiation of the water phantom the beam was turned off and a background spectrum was measured. The spectrum showed no germanium activation gamma lines; neither did the detector show any kind of energy disruption in the phantom measurement setup. The damages on the crystal are not always detectable as long as the cooling of the detector is sustained. When the detector later is cycled to room temperature and the cooled again the damages appear more prominent (ORTEC). When cycling the detector used in this experiment no irregularities in peak shapes could be noticed, neither could any other sign of damage such as poor vacuum or signal disruption be detected.
The lead shielding showed to be insufficient. The result of this presented was a large background in the measured spectrum. When investigated the side photon shielding showed to be the one failing. 3.5 cm was not enough and it needs to be reinforced to a minimum of 10 cm, perhaps 15cm. The 38 cm collimator serving also as shielding and

was working with no problems to attenuate frontal contributions to background originating from the phantom and neutron collimator.
Suggestions for improvement would be to increase the photon shield on the sides as explained above, in the rear of the detector and at the same time increasing the collimator hole diameter to a few centimetres. This would increase the signal-to-noise ratio and at the same time heavily suppress the background.

Monte Carlo Calculations

The computer calculations regarding geometrical efficiency showed unexpected accuracy compared to measurement results, this probably because of the high accuracy in the manufactured parts and control of environmental variables.

The relative efficiency measured and stated by ORTEC is 18%. When calculated by MCNP computer code the result obtained was 26% (+44% higher). This can be caused by a lot of different factors such as irregular crystal shapes and inhomogeneous electric field in the crystal caused not only by internal disturbing fields inside the detector, but external fields as well.

When using the neutron source in MCNP4C for calculation of the count rate and spectrum, the calculations suffered from very high uncertainties due to the original purpose of the source specification and MCNP geometry.
The count rate estimation results were not accurate. A count rate of 265 000 cps for 600 kW reactor power does not match 290 000 cps for 100 kW reactor power in the real measurements. In the MCNP geometry walls and surrounding material other than the beam collimator are excluded, cutting away a contribution to the spectrum. It would not be possible to include all this detail into the MCNP calculations.

Measurements

The test of geometrical efficiency with the small collimator showed a good resemblance between calculations and measured values. It also showed general characteristics of the function for the shield construction which was vital to know when the variable collimator was used in measurements at Studsvik. This information also proved to be vital in interpretation of the tomographical reconstruction as well.

The measurements inside the treatment room showed unexpected high background but contributed to an understanding of how to conduct this type of measurements. This was a choice of testing a modifiable system, a trial and error approach instead of trying to theoretically estimate all details. In this case the approach seemed reasonable since a theoretical approach would have consisted out of many uncertainties. The background was not only a matter of distance to the phantom but also a matter of surrounding materials. The boron peak was found in analysis of the spectrum but the ratio net area/gross area needs to be closer to 1. At present time this ratio is closer to 0.01 revealing the problem with signal-to-noise ratio.
When the detector count rate rise above 140 000 cps and a critical dead time one need to adjust the electronics for higher count rates. This operation will decrease the energy resolution and the peak shape is altered. As a result of this operation the FWHM increases and summation peaks start to occur. The pulses that earlier was collected in a given interval is spread out over a larger interval than before and therefore the signal to noise ratio rapidly decreases.
These results showed that the trial and error method was a fast way to acquire the needed information to form a ground for an optimisation study.

The results from the tomographical setup showed potential in detecting activity concentration differences in different regions. However the activity ratio could not be recreated. The reasons to this mismatch in activity ratio were probably the combination of the following. Primarily, the sphere's projected area was fairly the same as the projected area of the collimator. From this, the lack of flatness in the centre regions of the projection could be expected. FWHM was only 16mm, also affecting the height and flatness, adding noise to the regions in the image that has great variance of pixel values. A more correct estimate of the activity ratio would be achieved by using a larger ^{131}I hot spot volume. Better results would also be achieved using a cubic shaped phantom and hot spot.
One must also keep in mind the limitations of the reconstruction algorithm. The FBP image contains a lot of noise, this probably because of the chosen filter. A standard filter of Butterworth type was used with different heights and shapes of the slope. No significant differences could be produced and a standard model was chosen for the representation.
Due to the presets of the experiment the MLEM algorithm was not attenuation corrected. This would bring up the deep sited voxel values from each projections point of view, and in this case add to higher image activity ratio.
An increased number of angles could have presented a result with better accuracy. A decrease of the number of angles from 16 to 8 lead to less image quality but still the image contours was visible.
The tomographical images are shown without histogram averaging.
This experiment focused on producing images of what is above referred to as hot spots. One must not forget that it might be possible to determine cold spots as well. Cold spots would in this case be volumes in the patient that does not accumulate boron well. These cold spots can also contain high scientific values in evaluation and development of this treatment. However this needs to be further evaluated.

Conclusions

The detector was functional up to 100 kW nominal reactor power and showed that the basic design of this PGS system operates in this kind of measurement situation. The photon shielding did not sufficiently enough suppress the photons entering the sides of the shielding and this resulted in a very small signal-to-noise ratio. The design of the system was constructed in such a way that improvements to the shielding structure are easily added, and this is needed to be able to continue performing studies using this PGS system. When the photon attenuation issue has been solved other materials with higher attenuation coefficients can be used to bring down the dimensions of the shielding. Perhaps a different choice of HPGe-detector with less relative efficiency, ~5% and different crystal shape would fit the task better. A different detector would not solve the background issue but will allow higher photon fluence through the detector and thereby allowing the PGS-system to measure at higher nominal reactor power.
The boron peak that is present in the reported measurements is small but has been measured in a treatment representative situation. When photon background is later suppressed a more certain boron peak area estimation can be performed. This will also allow a narrower field of view, and will perhaps also bring down measurement times.
The study regarding tomographical images showed possibilities in making images that could be useful for example in estimations regarding boron distributions and treatment development. If needed the length of the detector and shielding can be shortened by partial rebuilding of the equipment. Then a tomography equipment construction can be fitted in the treatment room. The weight of the design is not yet a problem and will be well in the range of what is possible to handle mechanically. Since only 180° of

rotational space was needed, initial testing with tomographical imaging in a BNCT treatment situation could be done in the future.

Acknowledgements

The author would first of all like to thank the supervisors Crister Ceberg and Per Munck af Rosenschöld for guidance through this whole work, since this thesis became a mixture between many different areas of expertise.
I would also take the opportunity to thank Jan Hultqvist and Lars Andersson-Ljus at the radiation treatment workshop, Lund university hospital, for their always open minded attitude to problematic designs.
I would also like to thank David Minarik for his excellent help in the image reconstruction area and his good taste for hard rock music.
I would like to thank Jan Fredin and his colleagues a Teknodont AB in Malmö for the help of making the Lithium plastic components for the neutron shielding.
Thanks to Erik Larsson for help with the MCNP computer code.
I also would like to thank Christer Samuelsson for the help regarding HPGe detector characteristics.
Last I would like to thank my girlfriend, family and friends for discussions and support through all moments of the work, thank you!

Carl Östlund

En smygtitt på det okända

Idag behandlas de flesta patienter som diagnostiserats med gliom, en otäck hjärntumör, med fotoner producerade i en linjäraccelerator på någon av landets strålbehandlingskliniker. Tumören växer inuti hjärnan på ett mycket aggressivt sätt, vilket gör den nästan omöjlig att bota. Det normala är att strålningen kombineras med cellgifter och kirurgi för att ge patienten så lång tid som är möjligt, till att leva ut återstoden av livet med så hög livskvalitet som möjligt. Behandlingen är mycket krävande både från patientens och från familjens synvinkel. Det finns alternativ till denna behandling och en av dessa är BNCT, vilket står för Boron Neutron Capture Therapy, bor neutron-infångnings-terapi. Detta är en typ av strålterapi där patienten bestrålas med neutroner istället för fotoner. Neutronerna bromsas in i patientens huvud genom att kollidera och studsa runt mot de andra atomerna, främst väte som finns i hjärnan. När de närmar sig stillastående öppnas en ny möjlighet i neutronen värld, nämligen den att förena sig med en annan atom. Det är olika sannolikhet att detta skall hända för olika atomer, men det är mest sannolikt för en boratom. När en bor-10 atom absorberar en neutron, så kommer detta att innebära att den nya atomen bor 11, blir instabil och sönderfaller nästan omedelbart. Den delas i två delar, en heliumatom och en litiumatom. När atomen klyvs frigörs en massa energi som får de två atomfragmenten att plöja likt meteorer genom cancercellen och där orsaka stora skador. Eftersom att man befinner sig några meter från en kärnreaktor och utnyttjar neutronerna från uranet som klyvs, så är detta en otroligt krävande miljö för den känsliga detektorutrustning som införskaffats till detta ändamål. En konstruktion av en specialinneslutning av detektorn i egentillverkad litiumplast och en hel del bly gör det möjligt att mäta ett begränsat område på ett mycket nära avstånd intill patienten.
När bor-11 atomen klyvs så meddelas detta till omvärlden genom att den sänder ut en foton med energin 478 keV. Innan en behandling får patienten via infusion i blodet en molekyl som till stor del tas upp av tumören. Eftersom att det är otroligt svårt att veta hur mycket bor en patient har i sin tumör utan att ta ett vävnadsprov från tumören, så har tankarna riktats åt att försöka mäta hur många fotoner med energin 478 keV som sänds ut från patienten under en bestämd tid. Detta för att sedan kunna uppskatta totala antalet klyvningar och sedan överföra detta till vilken stråldos från klyvningarna som har givits tumören. Behandlingen är en engångsbehandling som utförs en tid efter operation där man försöker ta bort så mycket som möjligt av tumören. Metoden och grundstenen i mitt examensarbete är att man under själva behandlingen riktar ett speciellt framtaget detektorsystem mot huvudet och mäter ovan nämnda fotoner från en del av patientens skalle. Systemet har utvecklats genom att använda datorer och speciella beräkningsprogram. Detta har gjort det möjligt att till viss del förutsäga detektorsystemets funktion och gensvar under bestrålning av en patient. Därmed finns det goda möjligheter att få mycket ny information om patientens behandling. Idag uppskattar man dosen i BNCT-behandlingen med ett blodprov som med mycket begränsad noggrannhet kan berätta vilken koncentration bor patienten hade i hjärnan under behandlingen. Men varför nöja sig med ett uppskattat medelvärde för hela skallen när möjligheten till noggrannare dosbestämning i själva tumören skymtar vid horisonten? Metoden öppnar en ny dimension för en denna alternativa behandling som i framtiden kan visa sig bättre än standardalternativet. Idag har metodutvecklingen kommit till det stadium att man kan mäta i behandlingsrummet på större delen av skallen. Ett fingeravtryck från boret framträder i det spektrum detektorn mäter. Genom en finurlig lösning i detta examensarbete kan vi nu bryta de gamla banor som tidigare hindrat utvecklingen. Patienterna kan därmed få en mer skräddarsydd behandling i realtid styrd av patientens individuella borupptag i tumörregionen. Tekniken har inte tillåtit oss att göra sådant tidigare, nu tar vi oss friheten till en smygtitt på det okända.

Handledare: **Crister Ceberg, Per Munck af Rosenschöld**

Reference List

Asbury, A. K., et al. "Neuropathologic study of fourteen cases of malignant brain tumor treated by boron-10 slow neutron capture radiation." J.Neuropathol.Exp.Neurol. 31.2 (1972): 278-303.

Capala, J., et al. "Boron neutron capture therapy for glioblastoma multiforme: clinical studies in Sweden." J.Neurooncol. 62.1-2 (2003): 135-44.

Ceberg, C. P., et al. "Performance of sulfhydryl boron hydride in patients with grade III and IV astrocytoma: a basis for boron neutron capture therapy." J.Neurosurg. 83.1 (1995): 79-85.

Coderre, J. A., et al. "Neutron capture therapy of the 9L rat gliosarcoma using the p-boronophenylalanine-fructose complex." Int.J.Radiat.Oncol.Biol.Phys. 30.3 (1994): 643-52.

Coderre, J. A., et al. "Biodistribution of boronophenylalanine in patients with glioblastoma multiforme: boron concentration correlates with tumor cellularity." Radiat.Res. 149.2 (1998): 163-70.

Coderre, J. A., et al. "Derivations of relative biological effectiveness for the high-let radiations produced during boron neutron capture irradiations of the 9L rat gliosarcoma in vitro and in vivo." Int.J.Radiat.Oncol.Biol.Phys. 27.5 (1993): 1121-29.

Coderre, J. A. and G. M. Morris. "The radiation biology of boron neutron capture therapy." Radiat.Res. 151.1 (1999): 1-18.

EG&G ORTEC Catalog 97/98, Modular Pulse-processing electronics and semiconductor radiation detectors.

Elowitz, E. H., et al. "Biodistribution of p-boronophenylalanine in patients with glioblastoma multiforme for use in boron neutron capture therapy." Neurosurgery 42.3 (1998): 463-68.

Gilbert, M. R., et al. "A phase II study of temozolomide in patients with newly diagnosed supratentorial malignant glioma before radiation therapy." Neuro.-oncol. 4.4 (2002): 261-67.

Giusti, V., et al. "Monte Carlo model of the Studsvik BNCT clinical beam: description and validation." Med.Phys. 30.12 (2003): 3107-17.

Kobayashi, T., Y. Sakurai, and M. Ishikawa. "A noninvasive dose estimation system for clinical BNCT based on PG-SPECT--conceptual study and fundamental experiments using HPGe and CdTe semiconductor detectors." Med.Phys. 27.9 (2000): 2124-32.

Mukai, K., Y. Nakagawa, and K. Matsumoto. "Prompt gamma ray spectrometry for in vivo measurement of boron-10 concentration in rabbit brain tissue." Neurol.Med.Chir (Tokyo) 35.12 (1995): 855-60.

Munck af Rosenschold, P. M., et al. "Toward clinical application of prompt gamma spectroscopy for in vivo monitoring of boron uptake in boron neutron capture therapy." Med.Phys. 28.5 (2001): 787-95.

Nichols, T. L., et al. "Improved treatment planning for boron neutron capture therapy for glioblastoma multiforme using fluorine-18 labeled boronophenylalanine and positron emission tomography." Med.Phys. 29.10 (2002): 2351-58.

Ninth International Symposium on Neutron Capture Therapy for Cancer, October 2-6, 2000, NCT Osaka, Japan

Ono, K., et al. "Radiobiological evidence suggesting heterogeneous microdistribution of boron compounds in tumors: its relation to quiescent cell population and tumor cure in neutron capture therapy." Int.J.Radiat.Oncol.Biol.Phys. 34.5 (1996): 1081-86.

Palmer, M. R., et al. "Treatment planning and dosimetry for the Harvard-MIT Phase I clinical trial of cranial neutron capture therapy." Int.J.Radiat.Oncol.Biol.Phys. 53.5 (2002): 1361-79.

Research and development in Neutron Capture Therapy, Essen, 8-13, 2002, Wolfgang Sauerwein, Raymond Moss and Andrea Witting, International Proceedings division. ISBN 88-323-2909-3

Smith, D. R., et al. "Quantitative imaging and microlocalization of boron-10 in brain tumors and infiltrating tumor cells by SIMS ion microscopy: relevance to neutron capture therapy." Cancer Res. 61.22 (2001): 8179-87.

Verbakel, W. F. "Validation of the scanning -gamma-ray telescope for in vivo dosimetry and boron measurements during BNCT." Phys.Med.Biol. 46.12 (2001): 3269-85.

Verbakel, W. F., et al. "Towards in vivo monitoring of neutron distributions for quality control of BNCT." Phys.Med.Biol. 47.7 (2002): 1059-72.

Verbakel, W. F., et al. "Boron concentrations in brain during boron neutron capture therapy: in vivo measurements from the phase I trial EORTC 11961 using a gamma-ray telescope." Int.J.Radiat.Oncol.Biol.Phys. 55.3 (2003): 743-56.

Verbakel, W. F. and F. Stecher-Rasmussen. "On-line reconstruction of low boron concentrations by in vivo gamma-ray spectroscopy for BNCT." Phys.Med.Biol. 46.3 (2001): 687-701.

Verbakel, W. F. and F. Stecher-Rasmussen. "A gamma-ray telescope for online measurements of low boron concentrations in a head-phantom for BNCT." Nuclear Instruments and Methods in Physics Reasearch. A 394 (1997)163-172.